Metrological characterization of the GAMPIX gamma camera

Guillaume Amoyal, Vincent Schoepff, Frédérick Carrel, Valérie Lourenço, Daniel Lacour, Thierry Branger

Metrological characterization of the GAMPIX gamma camera

G. Amoyal[(a)], V. Schoepff[(a)], F. Carrel[(a)], V. Lourenco[(b)], D. Lacour[(b)], T. Branger[(b)]
[(a)] *CEA, LIST, Sensors and Electronic Architectures Laboratory (LCAE), CEA-SACLAY 91191 GIF-SUR-YVETTE cedex, France*
[(b)] *CEA, LIST, Laboratoire National Henri Becquerel (LNE-LNHB), CEA-SACLAY 91191 GIF-SUR-YVETTE cedex, France*

***Abstract*—Gamma imaging is a technique that allows the spatial localization of radioactive sources in decommissioning phases of nuclear facilities, nuclear waste management applications, radiation protection, and Homeland Security. One asset of this technique is the possibility to quickly localize radioactive sources associated with a quantitative information on their intensity. Using gamma camera diminishes the dose received by operators and consequently respects the ALARA principle ("As Low As Reasonably Achievable").**
For several years, CEA LIST has been designing a coded aperture gamma camera, called GAMPIX. This imager was industrialized by MIRION Technologies (CANBERRA) under the commercial name of iPIX. An extensive study was initiated to validate the GAMPIX quantitative performances for evaluation of dose rate and associated uncertainties. The validation was performed with single and multiple radioactive sources covering an energy range from 60 keV to 1.3 MeV. This article presents experimental results obtained with the GAMPIX gamma camera in the framework of the EMRP ENV54 METRODECOM project.

I. Introduction

Localization of radioactive hotspots is a major issue for several applications related to the nuclear industry (radiation protection measurements in nuclear power plants, decommissioning applications, post-accidental events like Fukushima) or Homeland Security applications and implies the use of transportable and easily deployable systems. Gamma cameras are powerful tools to address this remote localization challenge. These systems enable to superimpose a gamma-ray image with a visible image in order to locate radioactive hotspots present in their field-of-view. Compton or coded aperture gamma-ray imagers, with applications in nuclear industry, were developed by several research teams in the past years: the iPIX gamma camera, based on a CEA LIST technology and industrialized by Mirion Technologies under the commercial name iPIX [1]; POLARIS-H by H3D [2]; ASTROCAM 7000HS by Mitsubishi Heavy Industries [3]; and NUVISION by NUVIA [4].

In addition to the qualitative information provided by gamma cameras, a quantitative information on the dose rate generated by a given hotspot can be extracted from the gamma ray pictures. The latter can be very useful to define interventional scenarios for decommissioning operations and minimize the dose received by operators. For this reason, performances of gamma cameras according to the nature and geometry of the radioactive source need to be carefully evaluated to provide an accurate dose rate value. Accuracy and uncertainties associated to dose rates provided by gamma cameras were not extensively considered in the literature and are for this reason the main topic of interest of our study.

The METRODECOM project consisted in developing methods for the radionuclide characterization of different types of materials present on the site being decommissioned [5], [6]. Within the scope of this project, an extensive study was initiated to validate quantitative performances of the GAMPIX system in a metrological way. Different reference sources were especially produced by the Laboratoire National Henri Becquerel (LNHB), part of CEA LIST, responsible for the metrological radiological references in France and core partner of the project. For the purpose of this study, point and extended sources were produced to assess the GAMPIX's performances on a large range of applications. The purpose of this study is to check the capability of the GAMPIX gamma camera to localize radioactive sources and estimate their associated dose rate.
This article gives an overview of experimental results obtained in the frame of the project. First, the main characteristics of the GAMPIX gamma camera are reminded, the main specifications of the radioactive sources produced for this study are detailed, and the methodology is described. Then, experimental results obtained in the framework of this project are presented. Finally, future developments related to this topic will be emphasized at the end of the article.

II. Experimental configuration for the metrological validation of the GAMPIX system.

A. *The GAMPIX gamma camera*

The prototype of GAMPIX gamma camera developed by CEA LIST was used for this study [7]. The GAMPIX gamma camera is composed of three main components: the Timepix chip, a pixelated chip composed of 256×256 squared pixels (55 µm side) [8], hybridized to a 1 mm thick CdTe, which provides information about the energy of the incoming gamma-ray [9]; a MURA coded-aperture in tungsten alloy for the localization of the radioactive source, which rank is 7 and thickness is 4 mm [10]; and a USB module to enable plug-and-play connection of the gamma camera with the computer. MIRION Technologies (CANBERRA) industrialized the GAMPIX gamma camera under the commercial name iPIX (Fig 1) in 2015.

Fig 1. On the left: GAMPIX gamma camera prototype developed by CEA LIST. On the right: the industrial iPIX version commercialized by Mirion Technologies (CANBERRA).

In the context of specific experiments carried out during the project, the Timepix chip was used in Time-Over-Threshold (ToT) mode (time spent by pulses generated by charge preamplifiers over a user-specified threshold) to provide a spectrometric information using the same data as those considered for the localization step [9]. A ToT spectrum of a 74 MBq Am-241 source recorded with GAMPIX at 1 m for an hour is illustrated in Fig 2.

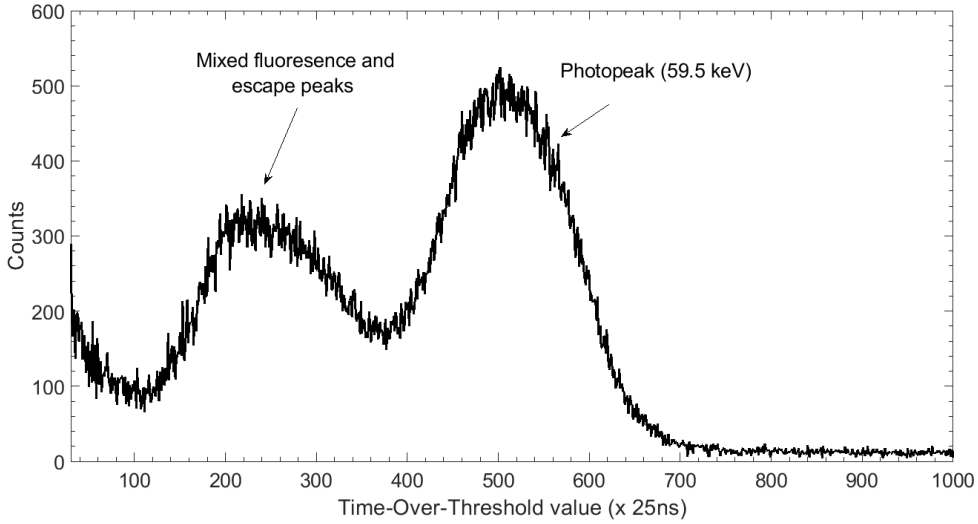

Fig 2. Time-Over-Threshold spectrum of a 74 MBq Am-241 source with GAMPIX. The distance between the source and GAMPIX is 1 m, and the measurement duration is 1 h.

B. Coded-aperture imaging technique with GAMPIX gamma camera and dose rate estimation

Gamma cameras with coded-aperture use a spatial modulation imaging technique. The coded-aperture, consisting of an array composed of opaque and transparent elements with a specific pattern, is placed between the radioactive source and the sensitive detection area. Photons emitted by a source object project on the sensitive detection area the pattern of the coded-aperture. This projection is called a shadowgram. The radioactive source is reconstructed in the decoded image by applying the knowledge of the coded-aperture pattern to the shadowgram [11].

In the case of the GAMPIX gamma camera, a MURA coded-aperture is used. The algorithm used to obtain the decoded image with GAMPIX is the method proposed in [10]. This method consists in an autocorrelation of the shadowgram with a decoding function represented by the coded-aperture pattern. The sensitive detection area (the Timepix detector) is composed of 256 × 256 squared pixels; therefore, the decoded image is composed of 256 × 256 pixels. In the decoded image, the radioactive source position, also described as the hotspot, corresponds to the position with the highest intensity. From the decoded image, the hotspot profile is extracted. Illustrations of a shadowgram, associated decoded image and hotspot profile are presented in Fig 3.

For a given measurement, the measured shadowgram corresponds to the energy deposited (expressed in ToT value) in each enlightened pixel of the sensitive detection area. Because of the coded-aperture thickness, self-vignetting in the coded-aperture has to be taken into account to estimate the dose rate when the radioactive source is off-centered [12]. The loss of sensitivity of GAMPIX depends on the radioactive source. For this reason, it is compensated with a correction matrix calculated for each radionuclide used in this study. The correction matrix associated with Am-241 and Cs-137 is illustrated in Fig 4.

The purpose of this study is to verify whether the intensity of the reconstructed hotspot is proportional to the dose rate of the radioactive source to be located. The dose rate is estimated as the integral of the hotspot profile divided by the time of measurement

for point sources, and of the surface for extended sources, to which the background noise is subtracted. For this reason, in the following figures, the value of the estimated dose rate is expressed in hotspot intensity unit, corresponding to the count rate in the reconstructed image.

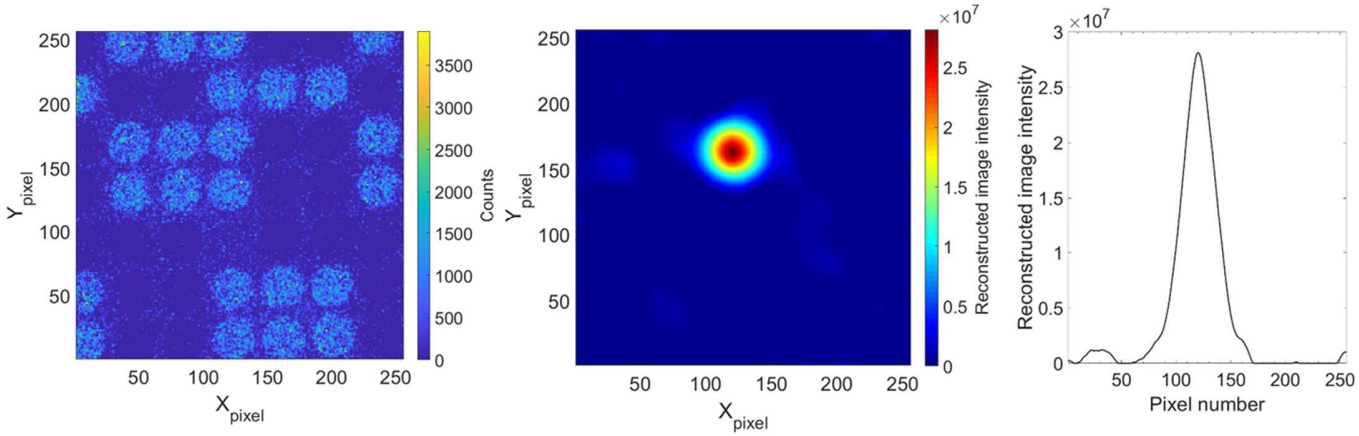

Fig 3. From left to right: illustration of a shadowgram measured with GAMPIX, the associated decoded image and the hotspot profile.

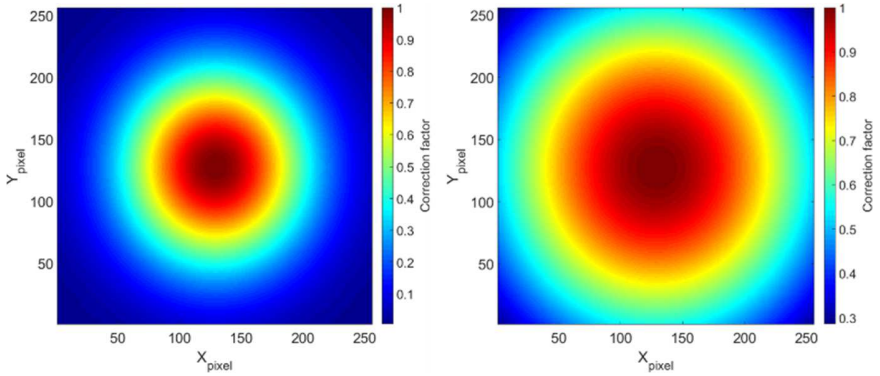

Fig 4. Correction matrix (applied to the decoded image) to compensate the loss of sensitivity of GAMPIX for Am-241 (on the left) and Cs-137 (on the right). Calculations for a MURA coded-aperture in tungsten alloy, rank 7, 4 mm thickness.

C. Specific METRODECOM radioactive sources

As part of the project, a set of specific point and extended sources was produced by the LNHB. Activities of the five reference Co-57 point sources range from 310 kBq to 5.33 MBq at the time of measurements. A single Am-241 point source was also produced with an activity of 1.14 MBq. High-energy gamma-ray emitters were also considered in this study: Cs-137 and Co-60, with activities starting from 1 MBq to 3 MBq. Three Cs-137 point sources and three Co-60 point sources were provided by the LNHB. In order to confirm the linearity of the hotspot intensity with the considered radioactive source activity, additional measurements were carried out for both radionuclides with higher activities. Those additional measurements were carried out with sources presenting the following characteristics: a 26 MBq Cs-137 source and a Co-60 source, both with a relative uncertainty of 15 %. Considering Co-57, the production of extended sources was achieved with a rectangular shape of 5x7 cm² dimensions for each extended source. Homogeneity of each extended source was checked using an auto-radiographer (10 minutes of exposure time), as illustrated in Fig 5, in which the red part represents the radioactivity distribution. Depending on the chosen mesh size (in orange: ~ 10 mm²; in green: ~ 40 mm²), the standard deviation of the activity distribution obtained was 13 % for the orange square and 9 % for the green square. The recommendations of [13] are followed during the calibration of the auto-radiographer. It was calibrated using point sources placed at 122 cm from the detector, over the whole energy range. Standard point sources are sealed using a 18 µm thick Mylar® sheet whereas the METRODECOM sources were covered with 125 µm Mylar® sheet. Corrections were performed at low energy to consider this extra absorption.

Six extended sources were used for this project, single or multiple extended sources measurements are carried out covering an activity between 143 kBq and 1.71 MBq.

The different sources designed by the LNHB cover an energy range from 60 keV (Am-241 sources) to 1.3 MeV (Co-60 sources). The set of radioactive sources used in this study cover the energy range of main nuclear emitters present during nuclear facility decommissioning, and have low relative uncertainties. Activities and associated uncertainties are presented in Table I for the different point sources; relative uncertainties correspond to a 95 % confidence interval; italic activities and uncertainties correspond to sources out of the scope of the METRODECOM project.

TABLE I
ACTIVITIES AND RELATIVE UNCERTAINTIES FOR THE POINT SOURCES DESIGNED BY THE LNHB (6/21/2016)

Radionuclide	Activity (MBq)	Relative uncertainty (k=2)
Co-57	0.31	1.5 %
	0.91	1.3 %
	1.62	0.90 %
	2.27	0.80 %
	5.33	0.60 %
Co-60	0.72	3.7 %
	1.49	3.6 %
	2.23	3.7 %
	4.76	*15 %*
Cs-137	0.76	3.6 %
	1.89	3.6 %
	2.83	3.6 %
	26.2	*15 %*

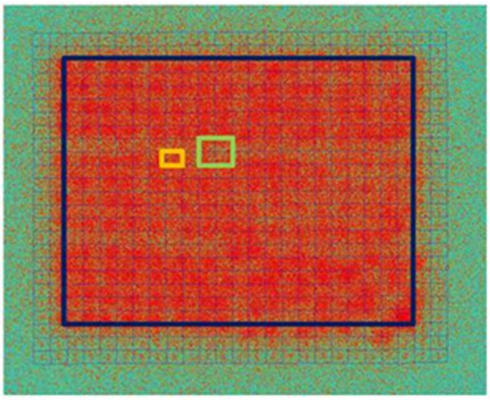

Fig 5. Radioactivity distribution (red) of an extended source obtained with an auto-radiographer (exposure time: 10 minutes). The standard deviation depends on the mesh size: 13% for the orange square (~ 10 mm²), and 9% for the green one (~ 40 mm²). The blue square corresponds to the real size and shape of the extended source (5×7 cm²).

D. Methodology

In order to ensure reproducibility and guarantee good counting statistics, a given measurement is composed of a set of acquisitions (at least 10 acquisitions). Each acquisition is composed of a given number of frames of 1 second (depending on the duration of the acquisition), and each frame is considered as independent. For each acquisition, the hotspot intensity is calculated, creating a distribution of hotspot intensities for each measurement. The normality of each hotspot intensities distribution is checked with the Shapiro-Wilk test [14]. If the test is passed, the hotspot intensity for the considered measurement is the mean value of the associated hotspot intensity distribution, and the uncertainty is estimated as two standard deviations of the distribution. Subsequently, uncertainties and error bars presented in this article correspond to the confidence interval defined in (1). In such a confidence interval, μ corresponds to the mean of the distribution, σ to the standard deviation, n is the size of the sample, and k is a coefficient corresponding to the confidence level.

$$\left[\mu - \frac{k\sigma}{\sqrt{n}}; \mu + \frac{k\sigma}{\sqrt{n}}\right], with\ k = 2 \quad (1)$$

III. EXPERIMENTAL RESULTS

A. Single point source

First, the metrological capability of the GAMPIX gamma camera was checked with single point sources. For these measurements, the GAMPIX gamma camera is placed in front (*i.e* on-axis) of the radioactive source at a distance of 1 m. The purpose is to confirm the linearity between the reconstructed hotspot intensity and the associated calibrated activity of the source. In this part, results obtained for measurements carried out with single Co-57, Cs-137 and Co-60 point sources are presented.

The evolutions of hotspot intensities in the decoded image according to the considered Co-57 source activities, Cs-137 source activities and Co-60 source activities are illustrated in Fig 6, in Fig 7 and in Fig 8 respectively. The response of the gamma camera is linear with the considered activity; however, the uncertainty on the hotspot intensity is important with the Co-60 sources. This high uncertainty is fully linked with the high energies of Co-60: 1.173 MeV and 1.332 MeV. Two aspects must be taken into account when considering the increase in uncertainties with Co-60 sources. First, the intrinsic detection efficiency of the Timepix detector is degraded when the energy of incident gamma-rays increases. Therefore, the number of hits in the measured shadowgram decreases, and so the associated uncertainty will increase. The second aspect concerns the coded aperture transparency. Those highly energetic gamma-rays are not fully stopped by the coded aperture reducing the signal-to-noise ratio (SNR) in the shadowgram, and consequently, increasing the uncertainty associated with the hotspot intensities.
Moreover, a slight offset in the linear fitting is observed for the different figures illustrating the hotspot intensity versus the calibrated activity of the considered radioactive source (Fig 6, Fig 7, Fig 8 and further on in this article for Fig 13, Fig 14, and Fig *15*). A hypothesis for this slight offset is the homogeneous background noise associated with the measurement, which affects the hotspot reconstruction.
Fig 9 illustrates the evolution of the relative uncertainty of the hotspot intensity for Co-57, Cs-137 and Co-60 sources according to the considered activities. The relative uncertainties are calculated from the results presented in Fig 6 for Co-57 sources, in Fig 7 for Cs-137 sources and in Fig 8 for Co-60 sources. As illustrated by Fig 9 and as expected, the higher the activity, the lower the relative uncertainty on the reconstructed hotspot intensity. For Co-57 and Cs-137 sources, a relative uncertainty lower than 5 % on the reconstructed hotspot intensity has been achieved. The same tendency can be expected for Co-60 sources (probably with a higher relative uncertainty on the reconstructed hotspot intensity), however the plateau has not been achieved, further measurements with higher activities are required. For radioactive sources with the same energy spectrum as the Co-57 or Cs-137, the relative error on the estimated dose rate is lower than 5%.

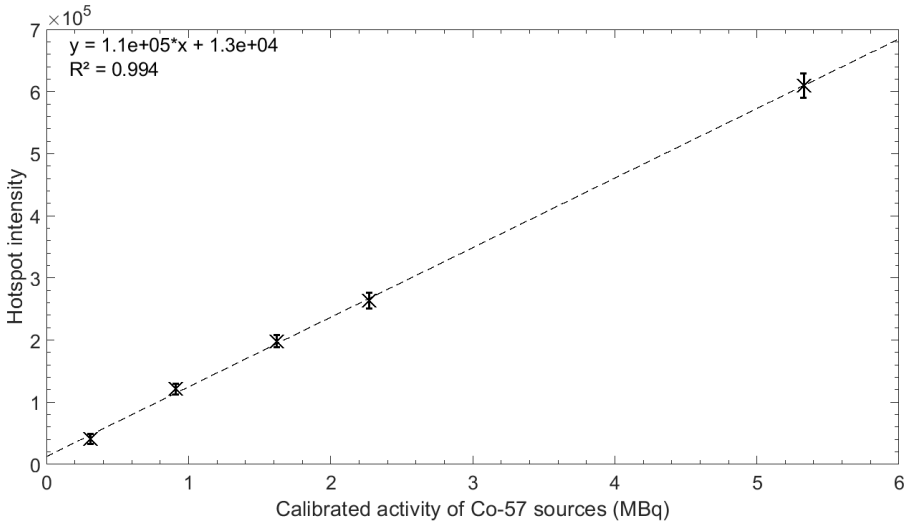

Fig 6. Hotspot intensities obtained with the GAMPIX gamma camera for Co-57 point sources of different activities.

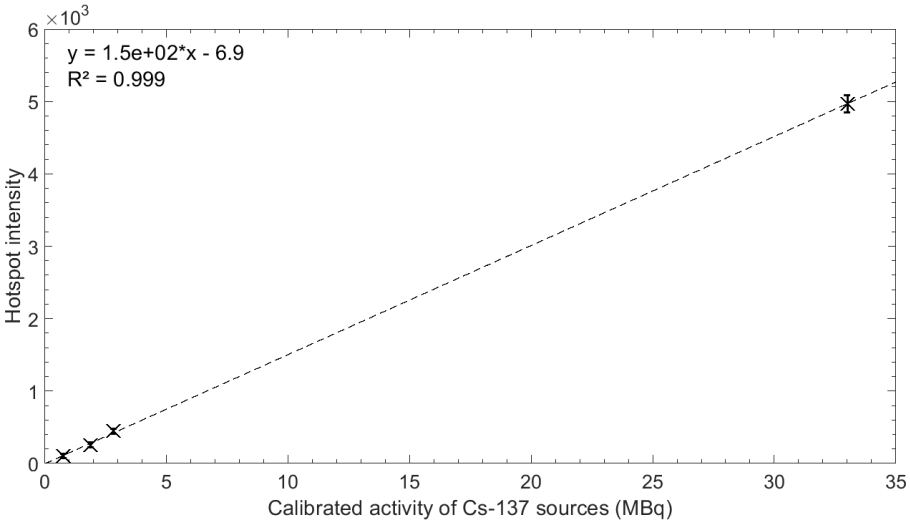

Fig 7. Hotspot intensities obtained with the GAMPIX gamma camera for Cs-137 sources of different activities.

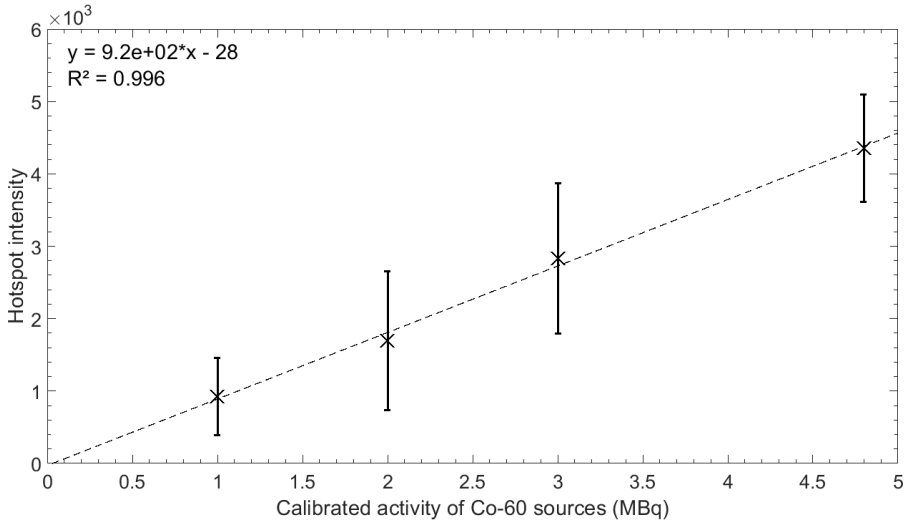

Fig 8. Hotspot intensities obtained with the GAMPIX gamma camera for Co-60 sources of different activities.

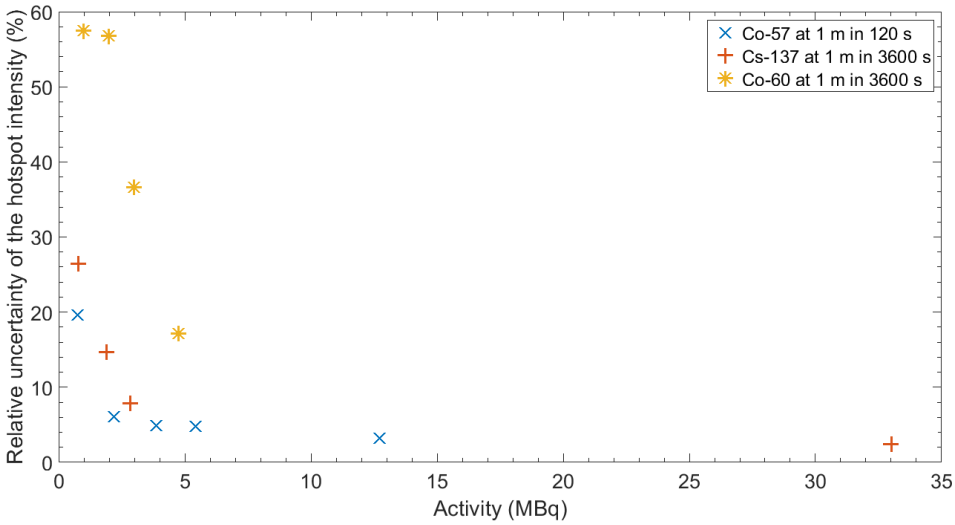

Fig 9. Relative uncertainty of the hotspot intensity for different radioactive sources at a distance of 1 m of the GAMPIX gamma camera for a measurement time of: 120 s for Co-57, 3600 s for Cs-137 and Co-60.

B. Multiple sources

In this part, results corresponding to measurements on multiple point sources are presented. Two configurations are studied: two Co-57 point sources with different activities for configuration 1; one Co-57 point source and one Am-241 point source for configuration 2. The experimental set-up is described in Fig 10: point sources are positioned simultaneously in front of the sensor. The distance between the sources is 30 cm in order to be separated with regard to the angular resolution of 6°. The distance between sources and the GAMPIX's sensor is 1 m.

The purpose of the experiments consists in assessing the metrological properties of the GAMPIX gamma camera with radionuclides of different activities on the first hand, and on the other hand with radionuclides of different nature.

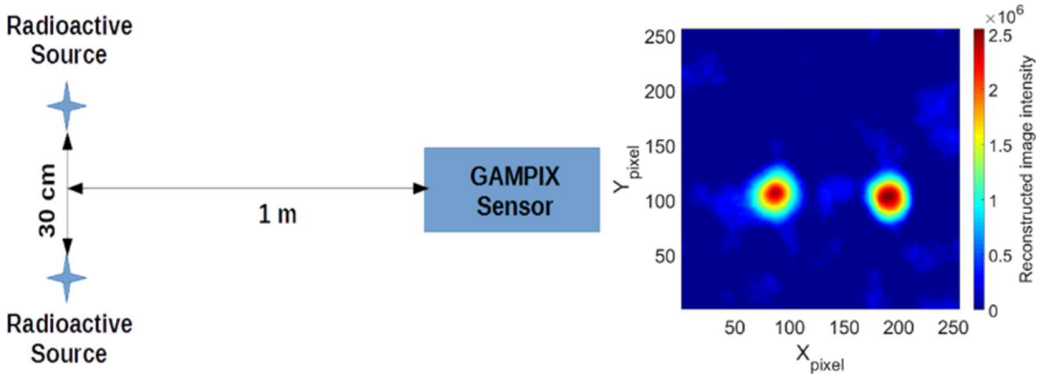

Fig 10. On the left: experimental set-up for multiple source measurements. On the right: decoded image from multiple source measurements.

Table 2 describes the different combination of Co-57 sources studied. Fig 12 shows results obtained for measurements on multiple Co-57 sources with different activities (configuration 1). It presents the ratio of hotspot intensities versus the ratio between calibrated activities of the two considered Co-57 sources. A linear behavior between the ratios of the calibrated activities and the hotspot intensities is observed, however the higher the ratio between source activities, the higher the uncertainty on the ratio between hotspot intensities. As shown in Fig 11, as the ratio between the calibrated activity increases, the source with the lower activity mixes up with the background noise, increasing the uncertainty of the associated reconstructed hotspot intensity. This phenomenon is directly linked with the decoding process.

TABLE II
COMBINATION OF CO-57 SOURCES ASSOCIATED WITH THE RATIO OF ACTIVITIES PRESENTED IN FIG 12

Calibrated activities of Co-57 sources (MBq)	Associated ratio
1.62 2.27	1.40
0.91 1.62	1.78
2.27 5.33	2.38
0.31 0.91	2.94
1.62 5.33	3.28
0.31 1.62	5.23
0.91 5.33	5.86

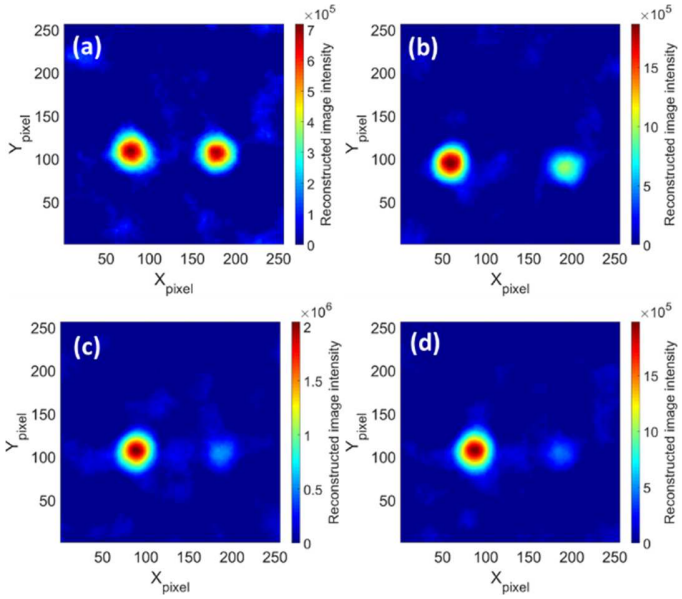

Fig 11. Decoded images with two sources of Co-57. On a) the ratio between source activities is 1.40, on b) 2.38, on c) 3.28 and on d) 5.86.

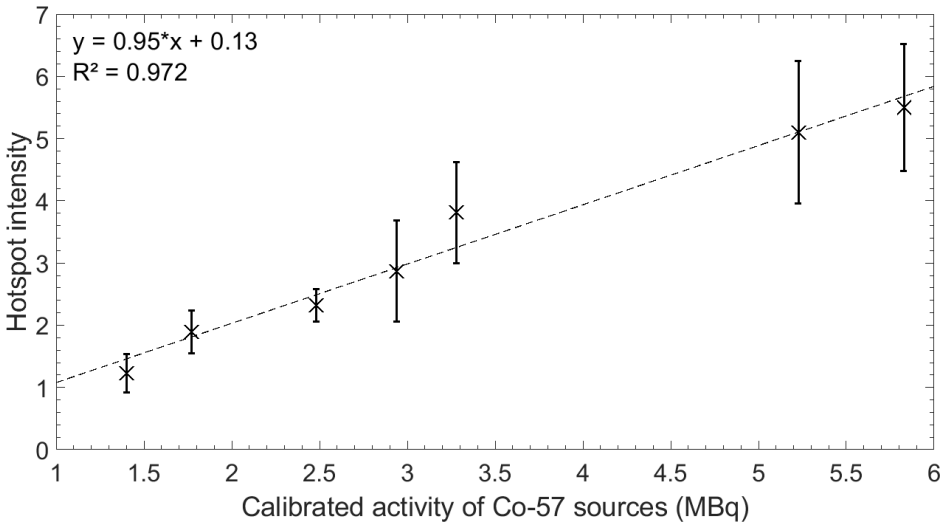

Fig 12. Configuration 1, ratio of hotspot intensities versus ratio between calibrated activities of Co-57 sources.

Experimental set-up for the second configuration is the same as the one described in Fig 10. Since only one Am-241 source is available, its activity is fixed, and measurements are realized for different activities of Co-57 sources. The first purpose of this measurement is to check whether the evolution of hotspot intensity for different sources of Co-57 is linear with the considered activity. The second purpose is to check if the hotspot intensity of the Am-241 source is constant with the variation of the activity of Co-57 sources.

The intensity of the reconstructed hotspot for Co-57 was found linear with the calibrated activity of Co-57 sources, as shown in Fig 13. Considering the hotspot intensity of the Am-241 source, the response of the GAMPIX gamma camera has the same order of magnitude, whatever the calibrated activity of Co-57 sources. However, the relative uncertainty on the hotspot intensity for the Am-241 increases with the activity of the Co-57 sources. Fig 14 shows the hotspot intensity of Am-241 source versus calibrated activity of Co-57 sources. The uncertainty degradation on the hotspot intensity of Am-241 source is due to the activity ratio between the sources. A solution to have a better separation between the two sources, and so a better hotspot intensity estimation, would consist in implementing energy criteria in the decoding process.

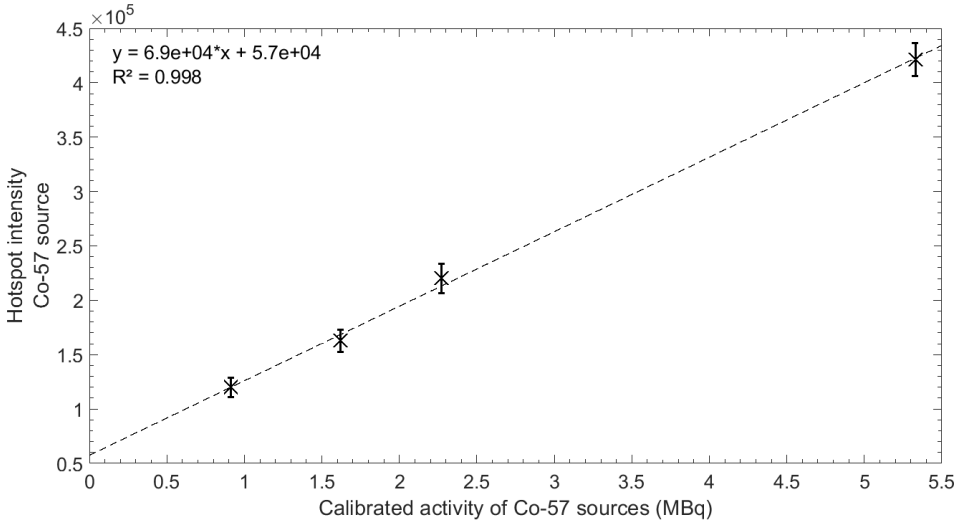

Fig 13. Configuration 2, hotspot intensity of Co-57 versus calibrated activity of Co-57.

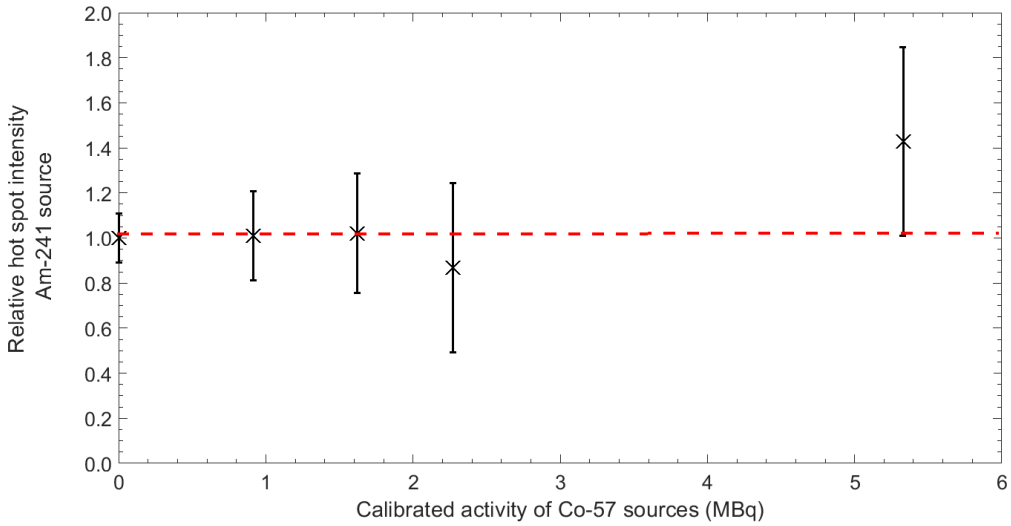

Fig 14. Configuration 2, relative hotspot intensity of Am-241 source versus calibrated activity of Co-57 sources. The reference hotspot intensity value (red dashed line) correponds to the Am-241 point source solely.

C. Extended sources

The linearity of the GAMPIX gamma camera was precisely checked with point sources. However many sources cannot be considered as punctual during in situ measurements (as waste barrels, contamination, tanks etc.). For this reason, the performances of the GAMPIX gamma camera response to extended sources have to be validated.

The purpose of these measurements is to check the evolution of the estimated dose rate with the considered activity on extended sources. Fig. 11 describes the calculated hotspot intensity for Co-57 extended sources as a function of the activity. Results show a linear response of the GAMPIX gamma camera. Additional measurements were carried out on extended sources with different shapes with a total activity of 1.714 MBq: one measurement on an extended source with a larger surface (10×14 cm²), and two measurements with the shape of a bent pipe from the side view and the frontal view corresponding to a more realistic situation of decommissioning, as illustrated on Fig 16. Table 3 summarizes results obtained for these measurements: the latter confirms that the hotspot intensities are similar for the different shapes. However, for a given activity, increasing the surface leads to higher relative uncertainties. This phenomenon is due to a reduction of the surface activity density when the surface increases. Moreover, when the surfaces increases, the self-vignetting of the mask increases, degrading the measurement.

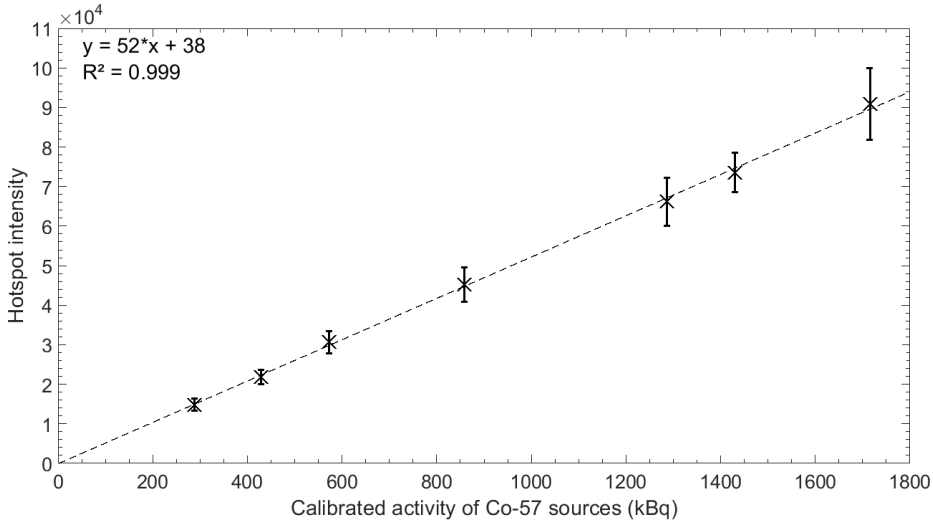

Fig 15. Hotspot intensities versus calibrated activities of Co-57 extended sources.

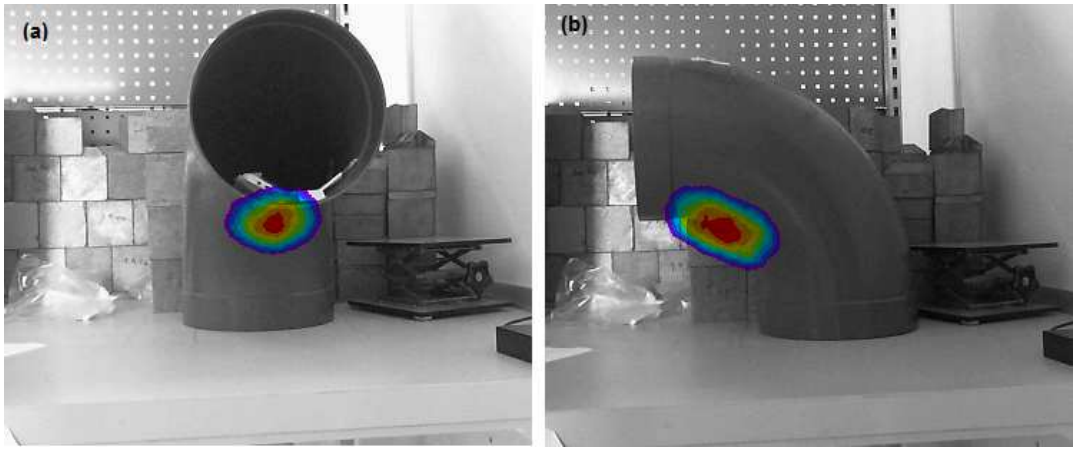

Fig 16. Superimposition of a visible image and a decoded gamma image. Measurement on Co-57 extended sources with an activity of 1.714 MBq placed in a bent pipe, frontal view (a) and side view (b).

TABLE III
COMPARISON OF THE HOTSPOT INTENSITIES FOR DIFFERENT SHAPES OF CO-57 SPREAD SOURCES (1.716 MBQ)

	Normalized hotspot intensity	Relative uncertainty (k=2)
Surface 5×7 cm²	1	4.5 %
Surface 10×14 cm²	0.98	12 %
Bent pipe Front view	0.97	13 %
Bent pipe Side view	1	14 %

IV. CONCLUSION AND FUTURE DEVELOPMENTS

This study was carried out in the framework of the European EMRP ENV54 METRODECOM project for decommissioning purposes. The objective of this study was to validate the metrological capabilities of the GAMPIX gamma camera to estimate the dose rate from reconstructed hotspots profiles. The set of nuclear sources used for this study was metrologically qualified by LNHB. During our trials, a satisfying reproducibility was observed for the different acquisitions obtained for a given experimental configuration.

It has been shown that the GAMPIX gamma camera can localize and quantify dose rate of single and multiple nuclear sources. The estimated dose and the associated uncertainties have been precisely qualified on a set of radionuclides. This qualification has

been carried out on a set of nuclear sources that includes point sources, extended sources, and covers the energy range of radionuclides mainly encountered in nuclear industry (from 59 keV to 1.3 MeV). Results of this study prove the capability of the GAMPIX gamma camera to be used for decommissioning process in a quantitative way, which contain highly radioactive punctual hotspots (activation points, nuclear matter) and extended radioactive emitters (contamination, tanks…).

A relative uncertainty lower than 5 % on the estimated dose rate for Co-57 and Cs-137 sources (with the same energy spectrum as the radioactive sources used in this study) has been achieved. In order to have a better relative uncertainty on the estimated dose rate, adding a spectroscopic information in the decoding process is required. This will be realized within the scope of the EMPIR program, through the ENV09 METRODECOM II project. This project consists in a metrological characterization of the spectrometric response of gamma imagers, including the GAMPIX gamma camera.

ACKNOWLEDGMENTS

This work was partially funded by the European Commission and EURAMET under the EMRP Project reference ENV54 METRODECOM.

REFERENCES

[1] K. Amgarou, A. Patoz, D. Rothan, and N. Menaa, “iPIX: A New Generation Gamma Imager for Rapid and Accurate Localization of Radioactive Hotspots,” no. October, pp. 3–5, 2014.

[2] C. G. Wahl *et al.*, “Polaris-H measurements and performance,” *2014 IEEE Nucl. Sci. Symp. Med. Imaging Conf. NSS/MIC 2014*, 2014.

[3] D. Matsuura, K. Genba, Y. Kuroda, H. Ikebuchi, and T. Tomonaka, “" ASTROCAM 7000HS " Radioactive Substance Visualization Camera,” *Mitsubishi Heavy Ind. Tech. Rev.*, vol. 51, no. 1, 2014.

[4] G. Montemont *et al.*, “NuVISION: A Portable Multimode Gamma Camera based on HiSPECT Imaging Module,” *2017 IEEE Nucl. Sci. Symp. Med. Imaging Conf. NSS/MIC 2017 - Conf. Proc.*, pp. 6–8, 2018.

[5] J. Suran *et al.*, “Metrology for decommissioning nuclear facilities: Partial outcomes of joint research project within the European Metrology Research Program,” *Appl. Radiat. Isot.*, vol. 134, pp. 351–357, 2018.

[6] “EMRP ENV54 METRODECOM.” .

[7] F. Carrel *et al.*, “GAMPIX: A new gamma imaging system for radiological safety and homeland security purposes,” *IEEE Nucl. Sci. Symp. Conf. Rec.*, pp. 4739–4744, 2012.

[8] X. Llopart, R. Ballabriga, M. Campbell, L. Tlustos, and W. Wong, “Timepix, a 65k programmable pixel readout chip for arrival time, energy and/or photon counting measurements,” *Nucl. Instruments Methods Phys. Res. Sect. A Accel. Spectrometers, Detect. Assoc. Equip.*, vol. 581, no. 1–2, pp. 485–494, 2007.

[9] J. Jakubek, “Precise energy calibration of pixel detector working in time-over-threshold mode,” *Nucl. Instruments Methods Phys. Res. Sect. A Accel. Spectrometers, Detect. Assoc. Equip.*, vol. 633, no. SUPPL. 1, pp. S262–S266, 2011.

[10] S. R. Gottesman and E. E. Fenimore, “New family of binary arrays for coded aperture imaging,” *Appl. Opt.*, vol. 28, no. 20, p. 4344, 1989.

[11] E. Caroli, J. B. Stephen, G. Di Cocco, L. Natalucci, and A. Spizzichino, *Coded aperture imaging in X- and gamma-ray astronomy*, vol. 45. 1987.

[12] P. M. Charalambous, A. J. Dean, J. B. Stephen, and N. G. S. Young, “Aberrations in gamma-ray coded aperture imaging,” *Appl. Opt.*, vol. 23, no. 22, p. 4118, 2009.

[13] M. C. Lépy, A. Pearce, and O. Sima, “Uncertainties in gamma-ray spectrometry,” *Metrologia*, vol. 52, no. 3, pp. S123–S145, 2015.

[14] S. S. Shapiro and M. B. Wilk, “An Analysis of Variance Test for Normality (Complete Samples),” *Biometrika*, vol. 52, no. 3/4, pp. 591–611, 1965.